ACS central science

http://pubs.acs.org/journal/acscii

Research Article

Structural Dynamics of RNA in the Presence of Choline Amino Acid Based Ionic Liquid: A Spectroscopic and Computational Outlook

Kiran Devi Tulsiyan, Subhrakant Jena, María González-Viegas, Rajiv K. Kar,* and Himansu S. Biswal*

Cite This: *ACS Cent. Sci.* 2021, 7, 1688−1697

Read Online

ACCESS | Metrics & More | Article Recommendations | Supporting Information

ABSTRACT: Ribonucleic acid (RNA) is exceedingly sensitive to degradation compared to DNA. The current protocol for storage of purified RNA requires freezing conditions below −20 °C. Recent advancements in biological chemistry have identified amino acid-based ionic liquids as suitable preservation media for RNA, even in the presence of degrading enzymes. However, the mechanistic insight into the interaction between ILs and RNA is unclear. To the best of our knowledge, no attempts are made so far to provide a molecular view. This work aims to establish a detailed understanding of how ILs enable structural stability to RNA sourced from Torula yeast. Herein, we manifest the hypothesis of multimodal binding of IL and its minimal perturbation to the macromolecular structure, with several spectroscopic techniques such as time-resolved fluorescence and fluorescence correlation spectroscopy (FCS) aided with molecular dynamics at microsecond time scales. Relevant structural and thermodynamic details from biophysical experiments confirm that even long-term RNA preservation with ILs is a possible alternative devoid of any structural deformation. These results establish a unifying mechanism of how ILs are maintaining conformational integrity and thermal stability. The atomistic insights are transferable for their potential applications in drug delivery and biomaterials by considering the advantages of having maximum structural retention and minimum toxicity.

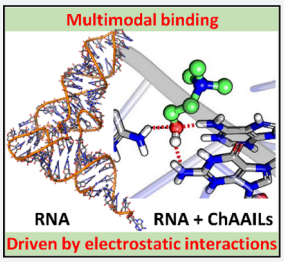

INTRODUCTION

RNA is a natural biopolymer with profound applications in medicine,[1] molecular or cellular biology,[2,3] and nano/biotechnology.[4] RNA is key to the central dogma of life in carrying the DNA blueprint and drives protein synthesis.[5,6] Besides serving as a component of the translation machinery, RNA also catalyzes chemical reactions and is instrumental in understanding disease biology.[7] Notably, to study RNA-associated processes, both *in vivo* and *in vitro*, the major challenge is their structural integrity in solution samples. This fundamental knowledge comes from their molecular architecture associated with the base pairing, electrostatic interactions, hydration capacity, and near environment effect, which requires harnessing to maintain RNA integrity during storage.[8] Cold storage is the commonly adopted method for RNA storage, in which samples are either stored at −20 °C to −80 °C or in liquid nitrogen.[9] During the past decade, new techniques have been developed for storing RNA at room temperature. Fabre et al. have shown that drying RNA samples and stabilizers can be stored at room temperature by using stainless steel capsules.[10] Reports by Seelenfreund et al. suggest desiccation as an efficient alternative for the preservation of RNA.[11] Moreover, silica encapsulation technology has also been emerging as a reliable method for the storage of RNA.[12] However, these technologies are obstreperous in nature, which comes with a high cost of maintenance.

On the other hand, ionic liquids (ILs) have recently gained interest, particularly for their role as efficient solvents to store biopolymers, proteins, and enzymes.[13−18] ILs are molten salts with low volatility, high ionic conductivity, and nontoxicity-like unique properties.[19−23] They can act as green alternatives to organic solvents for drug delivery and biochemistry applications.[18,24−27] Furthermore, they are suitable for long-term storage and extraction of macromolecules.[15,28−30] The suitability of ILs for storing proteins and DNA is widely practiced since these macromolecules can retain their functionalities.[31−36] However, in the case of RNA, their high vulnerability to degradation with external factors like temperature, pH, and enzymes pose a difficult task to store them for an extended period.[37] The advancement in finding a nontoxic and biocompatible solvent for RNA also demonstrates that ILs could be adequate and effective substitutes. Mamajonav et al. demonstrated the structural stability of nucleic acids in deep eutectic solvents (DES) and room temperature ILs (RTILs).[38] Mazid et al. investigated the role of ILs containing choline dihydrogen phosphate in the stability of siRNA in the presence of RNase A.[39] This was also supported by Fister et al. through their work on the RNA isolation from viruses using imidazolium and ammonium-based ILs.[22] A report by Pedro et al. also illustrates that choline-based ILs are suitable for preservation of recombinant RNAs.[40] Quental et al. successfully used amino acid-based IL solvents to extract and preserve

Received: June 26, 2021
Published: September 15, 2021

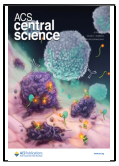

https://doi.org/10.1021/acscentsci.1c00768
ACS Cent. Sci. 2021, 7, 1688−1697

RNA.[41] Despite these findings, the principal mechanism that enables ILs suitable for RNA storage still remains underemphasized and unexplored. This work aims to traverse the mechanistic details through an assiduous analysis of spectroscopic measurements and theoretical modeling.

This is the first study that provides confirmatory spectroscopic evidence concerning the mode of interaction between choline amino acid-based ILs (ChAAILs) and RNA, to the best of our knowledge. In general, RNA prefers the A-form in buffer whereas DNA commonly exists as the B-form. Nucleic acid structures are well-known to be perturbed due to external factors, including temperature and pressure, disturbing the structural conformation. While RNA is extremely sensitive to degrading enzyme (RNAase), it requires additional precautions and measures while handling compared to other nucleic acids. However, in the case of tRNA, the modification of nucleobases has a significant role in regulating the overall stability of the biomolecule.[42] We developed an initial hypothesis and gained atomistic details of such interaction using theoretical modeling techniques followed by classical simulations up to microsecond time scales. The spectroscopic attestation of RNA−IL interaction was demonstrated using various techniques such as steady-state absorption (UV−vis and CD) and emission, TCSPC integrated with femtosecond-fluorescence up-conversion, and fluorescence correlation spectroscopy (FCS). Isothermal titration calorimetry experiments were also carried out to provide thermodynamic insights on RNA−ILs binding. RNA melting experiments were performed to get a comprehensive picture of the thermal stability of RNA in the presence of ILs.

RESULTS AND DISCUSSION

This work aims to investigate the structural insights from the interaction pattern and dynamics between RNA and ILs. Our focus is to explore (i) the site preference of ILs onto the macromolecular structure of RNA, (ii) dominant forces (electrostatic and van der Waal forces) that stabilize the complexes, (iii) physical stability, and (iv) effect of ILs on structural dynamics. Herein, we have adopted a combined computational and experimental approach to achieve the objectives mentioned above.

Binding Site Preference of ILs onto RNA Macromolecules. Molecular docking is used to explore the binding possibilities with their site preference based on the energetic evaluation. It forms the basis of our preliminary investigation to interpret the putative site of binding for the ChAAILs ([Ch][Glu] and [Ch][Asp]) with RNA. Initial calculations reveal that Ch binding preference is mainly onto the minor groove of the RNA structure, as shown in Figure 1A,B. However, there are no such site preferences for the counterion amino acids. The obtained binding energy of the docked complexes is ∼−4 kcal·mol^{-1}, irrespective of Glu and Asp. The orientation of the cholinium ion in the lowest energy conformation is stabilized through hydrogen bonding (Figure 1). The O−H group of the ligand is involved in H-bonding with nucleobases (O−H···N). In the case of DNA, a previous study has shown that Lennard-Jones (LJ) potential between ILs and DNA contributes to −10 to −23 kcal·mol^{-1} to the overall stabilization energy. However, our results for RNA show the LJ contribution is minimum (−1 to −2 kcal·mol^{-1}), indicating that there is feeble hydrophobic interaction between the ILs and RNA. Furthermore, we compared our docking results with the ethidium bromide (EB) molecule, which is also known to bind preferably at the minor-groove of nucleic acid structures, as shown in Figure 1C. Indeed, the lower energy conformation obtained also shows preference to the minor-groove location, like Ch, which further triggered us to verify this experimentally.

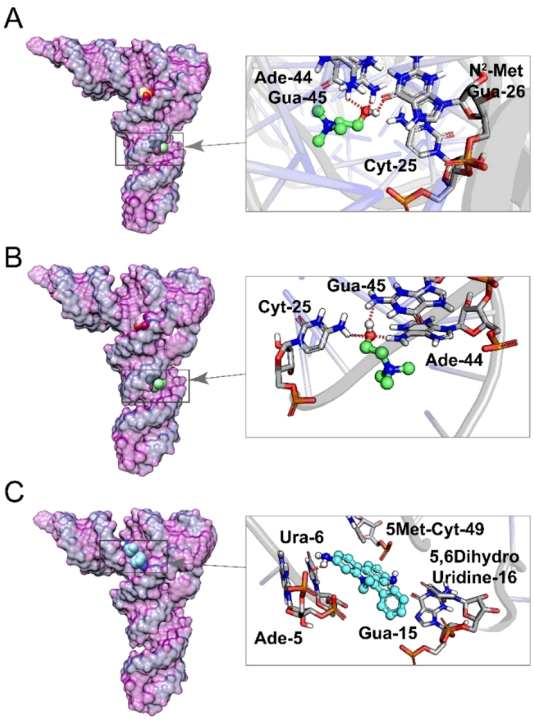

Figure 1. Starting structure of RNA complex with ChAAILs and EB: zoomed section of IL bound to macromolecule is shown for (A) RNA−[Ch][Glu] and (B) [Ch][Asp] and (C) zoomed-in section for RNA−EB.

Binding Mode Analysis with Absorption and Fluorescence Spectroscopy. UV−vis absorbance measurement is valuable for determining RNA purity and confirming the binding specificity of ILs. Since small molecule binding to RNA is possible through three modes, viz., intercalation, groove binding, or external binding, the change in absorbance and a shift in absorption maxima (λ_{max}) upon binding are good indicators.[43] A hyperchromic shift of the peak at 260 nm in the UV−vis spectrum of RNA−[Ch][Glu] and RNA−[Ch][Asp] was observed, which confirms a possibility of the presence of interactions between RNA and ILs (Figure 2A,B). Similar observations made by Dipak et al. are attributed to multimodal binding in nucleic acids.[33] The intercalation mode of EB binding to RNA was confirmed from the hypochromic and bathochromic shift (Figure S5A), which is in line with the previous report.[44] Further addition of IL to the RNA−EB complex resulted in hyperchromism at 280 nm, confirming the interactions present between RNA and ILs, whereas no spectral shift for the peak at 480 nm (which corresponds to the EB probe) attributes to the absence of interactions among ILs and EB. No complexation of EB with ILs was further confirmed from the minimal change in the absorption spectra of EB on the addition of ILs in the absence of RNA (Figure S5B). Similar observations are made with other fluorescent probes 4′,6-diamidino-2-phenylindole (DAPI) (Figure S5C,D).

As the RNAs have low fluorescence quantum yields, the fluorescence probes such as EB and DAPI are ideal and

https://doi.org/10.1021/acscentsci.1c00768
ACS Cent. Sci. 2021, 7, 1688−1697

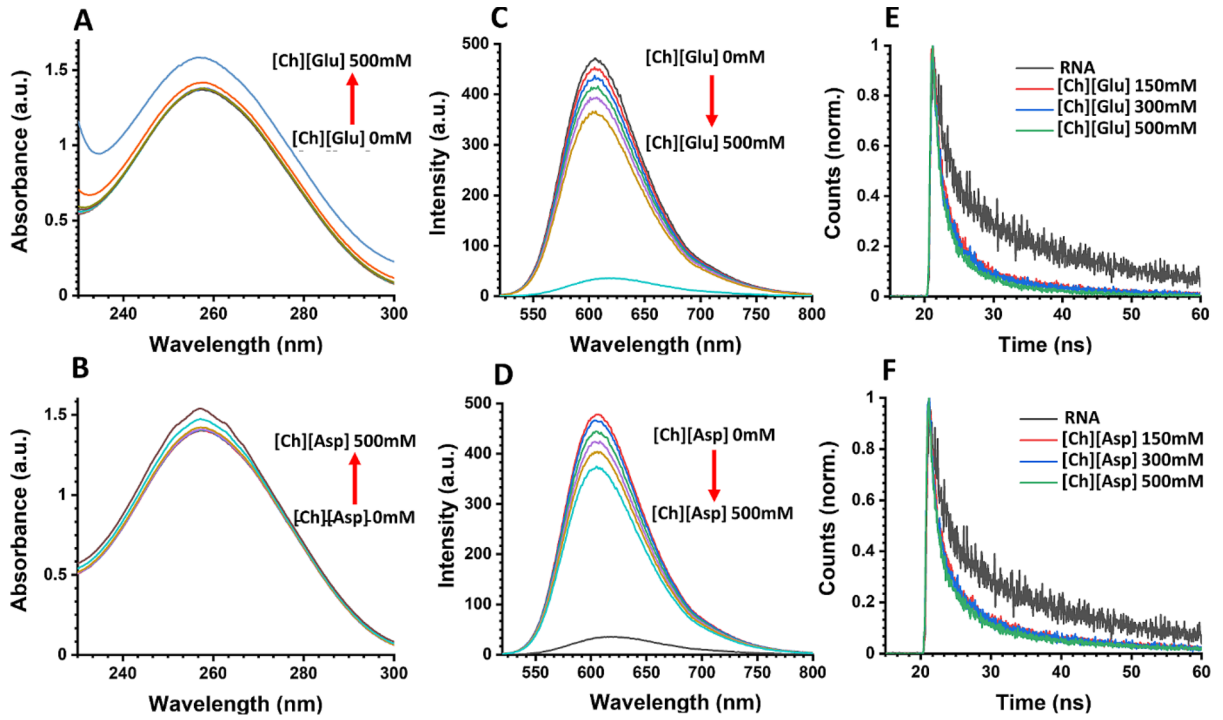

Figure 2. Spectroscopic characterization for binding studies between RNA and ChAAILs: (A,B) Steady-state absorption spectra of RNA with increasing concentration of [Ch][Glu] IL and [Ch][Asp] IL up to 500 mM, respectively. (C,D) Steady-state emission spectra of free EB, RNA bound EB, and EB-RNA complexed with increasing concentration of [Ch][Glu] IL and [Ch][Asp] IL, respectively. (E,F) Time-resolved fluorescence decay profiles of free EB-RNA in buffer and EB-RNA system in the presence of different concentrations of [Ch][Glu] IL and [Ch][Asp] IL, respectively.

Table 1. Fluorescence Decay Parameters[a] of Free EB, EB-RNA, and EB-RNA Complex in the Presence of Increasing Concentrations of ChAAILs

sample	IL-1 (mM)	IL-2 (mM)	τ_1 (ns)	τ_2 (ns)	τ_3 (ns)
EB	0	0	1.77(1.00)		
EB+RNA	0	0	1.96(0.07)	18.80(0.93)	
EB+RNA+IL-1	150		1.05(0.19)	18.77(0.42)	3.95(0.39)
EB+RNA+IL-1	300		1.08(0.23)	18.11(0.35)	4.18(0.42)
EB+RNA+IL-1	500		1.06(0.21)	18.69(0.34)	4.23(0.44)
EB+RNA+IL-2		150	1.04(0.22)	18.77(0.39)	3.95(0.39)
EB+RNA+IL-2		300	1.07(0.23)	18.11(0.37)	4.15(0.40)
EB+RNA+IL-2		500	1.06(0.24)	18.69(0.34)	4.20(0.42)

[a] a_i are the pre-exponential factors given in parentheses and represent the fractional contribution of each lifetime component.

valuable probes to investigate the structural dynamics of RNA through the steady-state and time-resolved fluorescence measurements. Thus, an optimization for the concentration of EB probes to attain maximum binding with RNA was necessary. First, fluorescence emission measurements were carried out by increasing the concentration of ILs. A gradual increase of both ChAAIL's concentrations resulted in a decrease in the fluorescence intensity of RNA (Figure 2C,D). Here the quenching is attributed to a direct displacement of EB by ILs from the RNA−EB complex. The corresponding Stern−Volmer plots obtained from the quenching studies of RNA binding to [Ch][Glu] and [Ch][Asp] give Stern−Volmer constant (K_{sv}) values of 0.00183 and 0.00194 mM^{-1}, respectively (Figure S6A), indicating that the binding strength of both ChAAILs is comparable. This further suggests that the cationic counterpart (Ch) has a significant role in binding, whereas the anionic counterparts bearing a similar polarizability value of 1.13 is expected to have a minimal effect on the binding and only contribute through charge stabilization. A similar observation for the other fluorescent probe (DAPI) that has groove binding with RNA confirms that ChAAILs have both intercalative as well as groove binding with RNA as ILs displace both the fluorescent probes (Figure S6B−D). These dye displacement results are in good agreement with previous reports where ILs are found to displace fluorescent probes efficiently. For example, Pabbathi et al. attributes the decrease in fluorescence intensity to the displacement of DAPI by morpholinium-based ILs in DNA and proposes that ILs have a multimodal binding with nucleic acids.[35] Another study by Dipak et al. on dye displacement also affirms that [Ch] can preferentially displace EB as well as DAPI from DNA.[33]

Though the interaction between ChAAILs and RNA happens in a shorter period (picosecond or nanosecond time scale regime), it is critical to get more insights on structural dynamics using the time-resolved fluorescence. Figure 2E

https://doi.org/10.1021/acscentsci.1c00768
ACS Cent. Sci. 2021, 7, 1688−1697

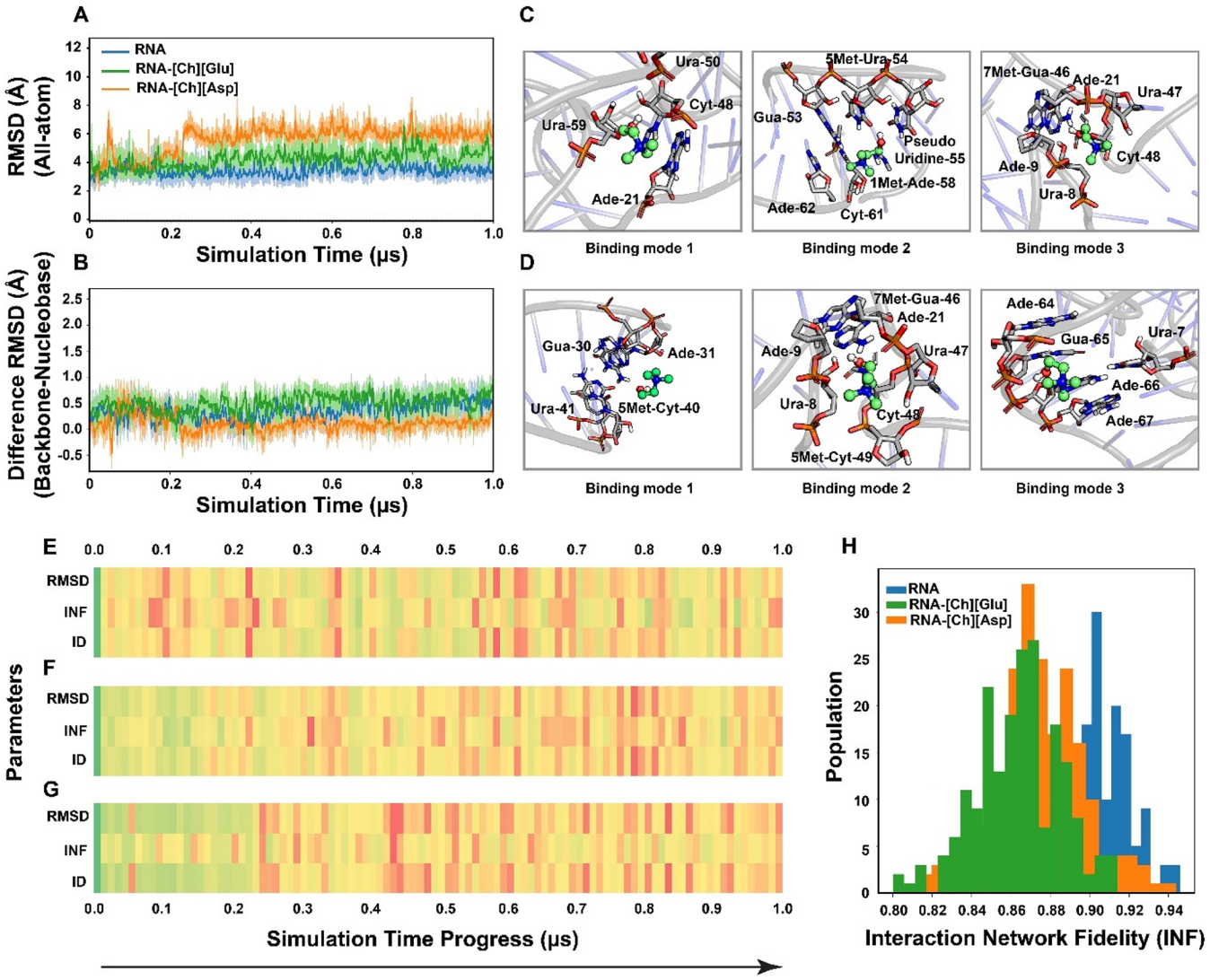

Figure 3. Binding analysis from ChAAILs interaction with RNA: (A) Time-dependent root-mean squared deviation (RMSD) analysis of equilibrated structures of RNA. (B) Difference RMSD between the backbone and nucleobase. Representation of RNA structure and putative binding of the [Ch][Glu] system (among the multiple binding pose found in trajectory) for (C) RNA−[Ch][Glu] and (D) RNA−[Ch][Asp]. Structural analysis of RNA across the simulation progress using the parameters RMSD, interaction network fidelity (INF), and deformation index (DI) for (E) RNA alone, (F) RNA−[Ch][Glu], and (G) RNA−[Ch][Asp]. The color scheme represents high (green) to low (red) values for INF, and opposite scheme for RMSD and DI. (H) Histogram plot to show the population of calculated INF values in three systems.

shows the fluorescence decay profiles for the RNA−EB complex in the presence of [Ch][Glu]. The decay of the EB probe follows a single exponential with a lifetime of 1.77 ns. However, in the presence of RNA, it decays biexponentially with a short (τ_1) and longer (τ_2) component of 1.97 and 20 ns, respectively. The corresponding amplitudes of these decays are 0.07 and 0.93 for free EB and RNA-bound EB. These findings are in good agreement with the report by Cui et al., which mentions a lifetime of 20.43 ns for the RNA−EB complex.[45] Nevertheless, our results confirm the maximum binding of EB to RNA. Upon addition of ILs, the fluorescence decay profiles can be fitted to triexponential. The third component confirms the complex formation with ILs. τ_1 and τ_2, in this case, are ∼1 and 18 ns, respectively, whereas the third component (τ_3) is ∼4 ns. The increase in the concentration of ILs results in a moderate increase in lifetime. Similar observations are made for [Ch][Asp] IL, shown in Figure 2F. Thus, the results are consistent among [Ch][Glu] and [Ch][Asp] (Table 1).

Thermodynamic Behavior of RNA. The thermodynamic behavior of RNA in the presence of ILs was analyzed using ITC. First, we titrated RNA against EB to determine its binding constant (K_b), which was found to be 4×10^4 mol^{-1} (Figure S7A). Next, the binding affinities of ILs with RNA were calculated by the same method. A higher concentration of ILs was required, owing to its smaller ionic size. The integrated heat data of RNA in the absence and presence of ILs with a single binding site model fitting ($\chi^2 = 0.97$) are provided in the Supporting Information (Figure S7B,C). Table S1 shows the thermodynamic parameters, indicating the K_b of [Ch][Glu] and [Ch][Asp] to be 0.4×10^3 and 0.6×10^3 mol^{-1}, respectively. These values are 100-fold less compared to the binding of EB with RNA. The free energies of binding (ΔG) are ∼−3.57 and −3.91 kcal·mol^{-1} for [Ch][Asp] and [Ch][Glu], respectively, which confirm that both ChAAILs are binding to RNA with equal strength.

Dynamic Insights of ChAAIL−RNA Interaction up to Microsecond Regime. In the above section, we recognized

https://doi.org/10.1021/acscentsci.1c00768
ACS Cent. Sci. 2021, 7, 1688−1697

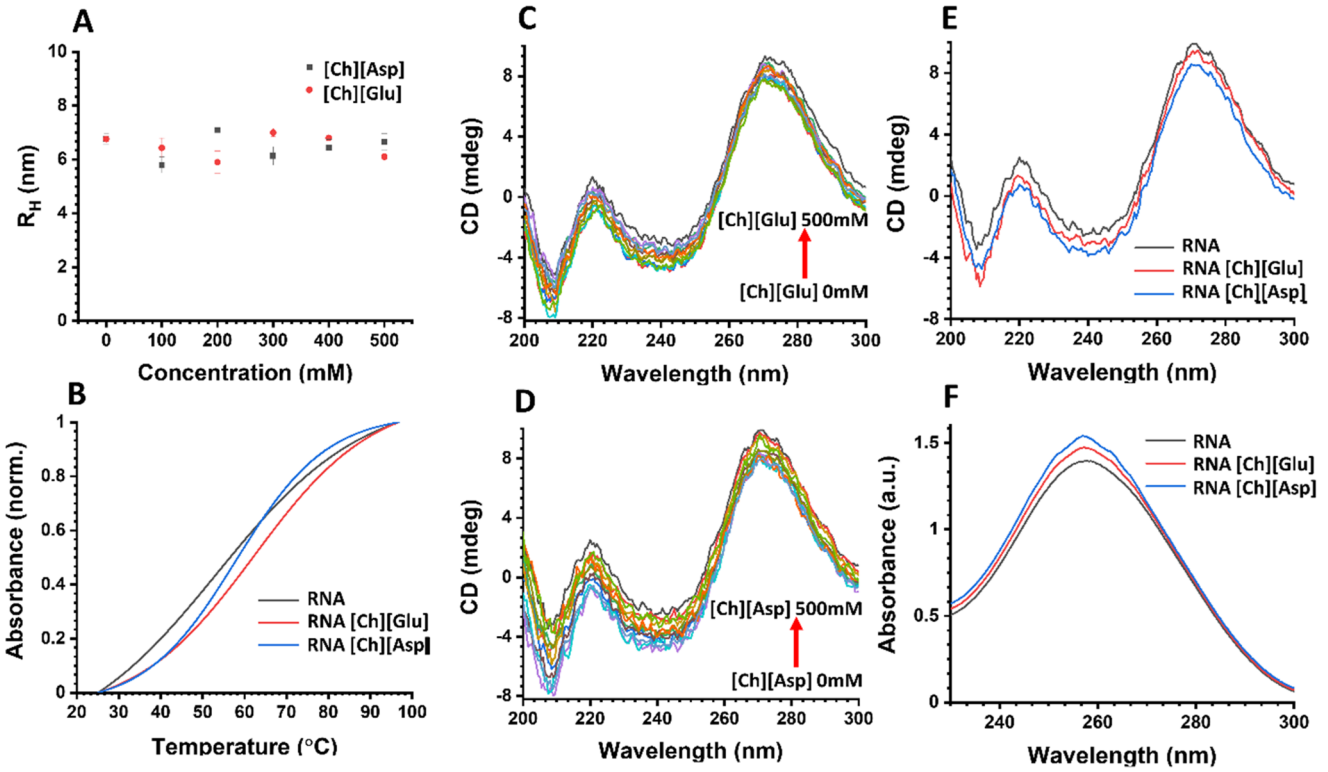

Figure 4. Structural stability and conformational analysis of RNA in the presence of ILs: (A) hydrodynamic radius (R_H) of RNA as a function of the concentration of [Ch][Glu] and [Ch][Asp] IL, (B) melting curves of RNA and RNA in 50 mM [Ch][Glu] IL and [Ch][Asp] IL, (C) CD spectra of RNA with increasing concentration of [Ch][Glu] up to 100 mM, (D) CD spectra of RNA with increasing concentration of [Ch][Asp] up to 100 mM, (E) CD spectra of preserved RNA samples in ChAAILs, and (F) absorption spectra of preserved and extracted RNA samples from ChAAILs.

the binding mode between ILs and RNA. The predicted binding free energies from the docking calculations are validated using ITC. However, detailed insight is necessary to reveal the dynamic pattern of such an interaction, which is possible using molecular dynamic simulations. This analysis uses trajectories of RNA−[Ch][Glu] and RNA−[Ch][Asp] of the 1 μs time scale. The corresponding root mean-squared deviation (RMSD) profiles are shown in Figure 3. The conformational dynamicity of RNA achieves states of equilibrium at the 0.3 μs time scale. Although RMSD shows a straight line (deviation <2 Å), it is necessary to compare the dynamic pattern of RNA in the absence of ILs.[46] A control simulation of RNA alone with an equivalent time scale shows that equilibration was achieved at the <100 ns time scale (Figure 3A,B). Furthermore, the deviation in the remaining time scale is comparable to that in the presence of ILs.

The binding preferences of cholinium cations are primarily in the minor groove region of RNA; however, we observed multiple (heterogeneity) binding poses. Different modes of [Ch] onto the RNA macromolecule can be visualized in Figure 3C,D. For the natural and modified nucleobase of RNA, we refer the readers to PDB code1EHZ. Additionally, to determine the global structural changes among the three simulation systems, RMSDs and interaction network fidelity (INF) are taken as a reference to calculate the deformation index (DI).[47] The mentioned parameters help to analyze the structural stability and packing of nucleic acid structures from the simulation snapshots.[48] A strong emphasis on these parameters in the context of three-dimensional RNA structures was discussed earlier by Parisien et al.[47] INF describes the conservation of base−base pairing and the stacking interactions. Identical conservation in successive snapshot scores as 1, whereas no conservation scores 0. In this concern, Kührová et al. reported INF as a reliable tool to determine the correct folding of RNA structures rather than RMSD.[49] The DI parameter accounts for both the RMSD and INF to evaluate the ratio between the structural dynamics and base-pair interaction. Figure 3 also shows the INF and DI values calculated for snapshots at an interval of 10 ns. A significant deviation in RNA structures occurs when they are with [Ch][Glu] and [Ch][Asp] (Figure 3F,G), up to a time scale of 0.25 μs, which is not present in the case of RNA alone (Figure 3E). Nevertheless, the qualitative pattern among both ChAAILs−RNA remains comparable. The INF value for the rest of the time scale remains within the range of 0.8−0.9 among the three systems. It also indicates no structural deformation or significant perturbation to the secondary structure of RNA in the presence of ILs.

Conformational Stability and Regeneration Study. Fluorescence correlation spectroscopic (FCS) studies were carried out to investigate the structural integrity of RNA in the presence of IL. FCS provides information about the hydrodynamic radius and diffusion time of the biomacromolecules. It is known that no significant perturbation tends to occur in DAPI-bound DNA structures in the presence of ILs.[35] In this study, we collected FCS data for DAPI and DAPI−RNA samples (see the methodology in the Supporting Information). The hydrodynamic radius (R_H) of RNA alone is estimated to be 7 ± 1 nm, which is in line with the reported data.[50−52] The R_H values in the presence of ILs are plotted against the

https://doi.org/10.1021/acscentsci.1c00768
ACS Cent. Sci. 2021, 7, 1688−1697

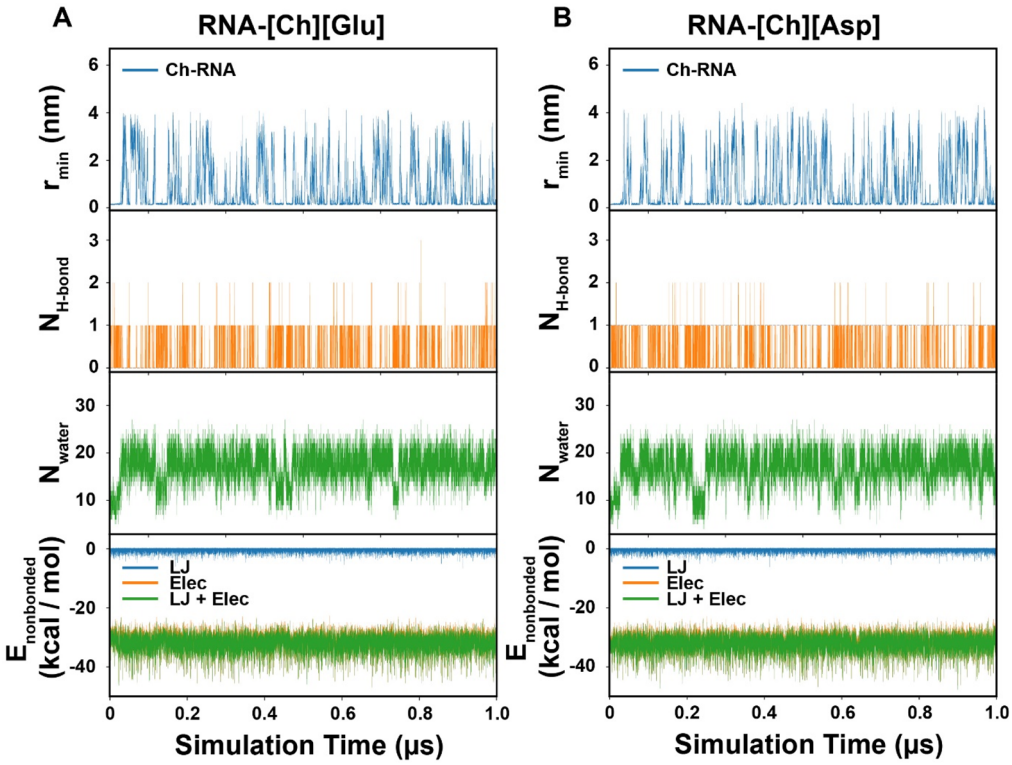

Figure 5. Dynamic insights from ChAAILs interaction with RNA: (A) RNA−[Ch][Glu] and (B) RNA−[Ch][Asp]. r_{min} denotes the proximal distance (nm units) between Ch and RNA, $N_{H\text{-}bond}$ represents the number of hydrogen bonds between RNA and Ch molecule, and N_{water} indicates the number of water molecules in the near shell of Ch molecule (0.3 nm). The energetics of interaction between Ch and the rest of the system is shown in terms of individual contribution (kcal/mol units) from Lennard−Jones (LJ) and electrostatic (Elec).

concentrations of ILs (Figure 4A). The R_H value does not change significantly with the increased concentration of IL. The correlation fluorescence data plots of DAPI−RNA and with ChAAILs are shown in Figure S8A−C. The experimental measurements can also be correlated using the gyration radius from theoretical calculations (Figure S9).

Analysis of the thermodynamic stability of RNA−IL binding was undertaken with the UV melting measurements.[53,54] Here, the increase in temperature is responsible for the release of stacking between nucleobases. It results in a strong-hyperchromic shift in absorbance spectra. The melting curves for RNA alone and in the presence of ChAAILs for absorbance at 260 nm are shown in Figure 4B. The melting temperature (T_m) of RNA is found to be 65 °C, which agrees with the reported literature.[53] The addition of ChAAILs leads to an increase in the T_m by 5 °C. The increase in T_m of RNA in the presence of ChAAILs indicates that RNA is more stable in the presence of ILs, which follows the previous reports by Pedro et al.[40] They showed that T_m of sRNA increases by almost 9 °C in the presence of Ch[DHP]IL, thus providing additional stability to RNA.[40] Similar observations were made by Quental et al. who observed additional stability to RNA by an increase in T_m ∼14 °C.[41] The INF analysis based on snapshots from MD simulations also reveals the differential behavior for RNA in the presence of [Ch][Glu] and [Ch][Asp] compared to RNA alone (Figure 3H). Such confirmation for the long-term stability of nucleic acid structures in the presence of Ch and imidazolium ILs binding with DNA is also reported based on MD simulations.[32] This increment in T_m is attributed to the fact that ILs add stability to the secondary structure of RNA. However, it also indicates the possibility of multiple binding poses because a single preference for groove binding cannot bring additional stabilization. Such observations are in line with the properties of DNA in the presence of ILs.[33]

The assessment of dynamic insights and structural perturbations is possible using CD spectroscopy. It is a well-known fact that the secondary structure of RNA has A-type double-stranded helices.[55] It gives a characteristic positive peak at 270 nm with a molar ellipticity of 9 mdeg and two negative peaks at 241 and 210 nm with a corresponding molar ellipticity of −2.5 and −5 mdeg, respectively. CD measurements of our sample with an increasing concentration of ChAAILs are shown in Figure 4C,D. No substantial changes occur in both the positive and negative peaks of RNA upon binding to ILs. It remains constant even after adding 500 mM IL, which provides additional validity that RNA structures retain their structural stability in ChAAILs. The minimal change in CD spectra in the presence of ILs is in good agreement with the previous reports,[33,40] where it is observed that ILs do not alter the conformation of nucleic acids. Using the same method, we further compare the CD spectra of stored and extracted RNA from the IL solution (after 3 weeks). Figure 4E shows that there is no change in the confirmation of extracted RNA.

The absorption spectra of the RNA sample extracted from the IL solution are shown in Figure 4F. The ratio between the absorbance at 260 and 280 nm confirms the stable conformation of the stored sample. These observations prove that no structural degradation or significant perturbation to the three-dimensional structure of the RNA happens in the solution containing ILs. This is also in good agreement with the observations made from the MD trajectories, with no

https://doi.org/10.1021/acscentsci.1c00768
ACS Cent. Sci. 2021, 7, 1688−1697

significant difference in RNA structures (RMSD and INF analysis, Figure 3) with and without ILs.

RNA−IL Binding Is Driven by Electrostatic Interaction. For additional insights into structural dynamics, we analuzed MD trajectories carefully. From the RMSD and base-stacking RNA analysis, no evidence is available to indicate any significant structural perturbations. The analyzed binding modes of Ch determine the proximal distance (min) between any atom of RNA and ligand (Figure 5), where min <0.4 nm represents a very close interaction between Ch and RNA. However, the fluctuation in the min distance denotes that ILs are interacting in several instances in the simulation. More evidence of binding between Ch and RNA is available through the number of hydrogen bonds. These hydrogen bonds are mostly forming between the positively charged Ch and the negatively charged phosphate group. These data also indicate a lower min value in simulation time because of one or more H-bonds. The water molecules present in the close shell of Ch also mediate the multiple binding poses with RNA. These observations are in good agreement with the experimental measurements. Further, we compared these data with the behavior of IL binding to DNA. In the case of RNA, we found that the binding is comparatively weak, as indicated by the binding free energy, H-bonds, and the r-min distance.

The energetic contribution analysis focuses on the non-bonded interaction between Ch and the rest of the system (RNA, water molecules, and counterions). The hydrophobic contribution (Lennard−Jones) in the Ch dynamics is negligible and appears as ∼−3 kcal·mol^{-1}. However, the driving force in these simulations is from the electrostatic interaction. Such energetic contribution accounts for ∼−35 kcal·mol^{-1}. This is obvious because the Ch binding is mainly through the H-bonding. Thus, we conclude that IL binding with RNA is not mediated through the surface-bound state but the groove-bound state. At the same time, the critical stabilization force is not through the hydrophobic and van der Waals forces. Our simulation results also confirm that the amino acid counterpart imparts no significant difference in the overall behavior. These observations agree with the observed spectral features from UV−vis, fluorescence, and CD spectroscopy.

Transferability of ILs−RNA Interaction for Potential Application. ILs are valuable alternatives compared to organic solvents due to their superior physiochemical properties like low toxicity, low chemical reactivity, high thermal stability, low inflammability, and high conductivity. Ch has been recognized as central to ILs due to the fact they are less cytotoxic, biodegradable, and easily synthesizable based on green chemistry.[56] On the other hand, a wide variety of anionic counterparts of ILs with Ch has been reported in conjunction with nucleic acids including chlorides, acesulfamates, and bis(trifluoromethylsulfonyl)imides;[57] imidazolium-based;[58] morpholinium-based;[35] pyridinium-based;[59] glycolate and pyruvate-based;[60] and glycolateacetate and dihydrogen phosphate.[61] Though all of these anionic counterparts have reported multimodal binding, they are not acceptable for routine use of ILs either due to expensive chemical route of synthesis, differential chemical stability, or being nonbiodegradable. Furthermore, the level of cytotoxicity is different, which otherwise is higher compared to AAILs.[62]

Note that long-term storage of RNA with marked extract efficacy is challenging and an evolving research field. Other than biochemical use, RNA also has potential pharmaceutical applications. For example, RNA robed with ammonium-based ILs are useful prodrugs for dermatological treatment.[63] It is evidenced that topical delivery of RNA using ammonium-based ILs have remarkable therapeutic efficacy.[64] Hence, ILs can also be useful drug delivery agents for RNA. Since ILs facilitate additional stability to RNA, they also can trigger a new direction for their use in the pharmaceutical and biotechnology research.

Besides ILs are salts with organic cations or anions, having irregular structure to delocalize their charges. The chemical shape of these molecules and low charges allow these molecules to (i) avoid tight packing during crystallization and (ii) acquire property of low melting points. Considering the amino acid-based ILs (AAILs), the important factor determining their efficacy is the polarity. Since this property determines the solubility of solute, miscibility with other solvents, and its reaction efficiency as a solvent, the polarizability of AAILs must be compared for their usefulness in specific applications. According to the Kamlet−Taft parameters for a series of AAILs, the polarizability ranges from minimum 1.04 [Val] to maximum 1.13 [Asp] and [Glu].[65] Thus, we hypothesized that AAILs irrespective of the amino acid counterpart could display identical behavior when used as a solvent medium for RNA.

CONCLUSION

The current work highlights the detailed mechanism responsible for the long-term storage of RNA by using ILs-based solvent medium. Herein, we elucidate the molecular-level understanding of the structural perturbation of RNA induced through choline amino acid-based ILs. The initial hypothesis for structural factors driving the interaction between ILs and RNA is obtained using computational modeling. The experimental validation of these findings is possible with suitable techniques such as steady-state fluorescence, UV−vis absorbance, circular dichroism spectroscopy, and isothermal titration calorimetry (ITC). Fluorescence correlation spectroscopy confirms that there is no change in the hydrodynamic radius of RNA in the presence of ILs, revealing the structural integrity of the biomolecule in the IL environment, which is further confirmed by circular dichroism analysis. UV−vis spectra analysis indicates multimodal binding of CAAILs with RNA, whereas dye displacement studies through fluorescence emission confirm IL molecules' intrusion into the minor groove of RNA.

Interestingly, we found that increases in IL concentration do not affect structural instability. From isothermal titration calorimetry and molecular docking, the binding energy of ILs with RNA is ∼−4 kcal·mol^{-1}, which indicates weak binding of ILs to RNA. Our results demonstrate that ILs preserve the structural integrity of RNA and are useful as nontoxic and biocompatible solvent. The lower binding energy of ILs with RNA further accounts for RNA extraction from the IL media. The significance of this study lies in the spectroscopic and theoretical evidence that noncytotoxic and eco-friendly ChAAILs are useful for the extraction and safe storage of RNA. The molecular-level information obtained from the present results can be valuable guidance for designing suitable ILs for the *in vivo* application of RNA.

https://doi.org/10.1021/acscentsci.1c00768
ACS Cent. Sci. 2021, 7, 1688−1697

■ ASSOCIATED CONTENT

Supporting Information

The Supporting Information is available free of charge at https://pubs.acs.org/doi/10.1021/acscentsci.1c00768.

Details of experimental and computational methods, NMR spectra, ITC isotherms, and safety statement (PDF)

■ AUTHOR INFORMATION

Corresponding Authors

Rajiv K. Kar − *Faculty II-Mathematics and Natural Sciences, Technische Universität Berlin, D-10623 Berlin, Germany;* orcid.org/0000-0003-4629-5863; Email: rajiv.k.kar@tu-berlin.de

Himansu S. Biswal − *School of Chemical Sciences, National Institute of Science Education and Research (NISER), 752050 Bhubaneswar, India; Homi Bhabha National Institute, Training School Complex, Mumbai 400094, India;* orcid.org/0000-0003-0791-2259; Phone: +91-674-2494 185/186; Email: himansu@niser.ac.in

Authors

Kiran Devi Tulsiyan − *School of Chemical Sciences, National Institute of Science Education and Research (NISER), 752050 Bhubaneswar, India; Homi Bhabha National Institute, Training School Complex, Mumbai 400094, India;* orcid.org/0000-0002-2325-560X

Subhrakant Jena − *School of Chemical Sciences, National Institute of Science Education and Research (NISER), 752050 Bhubaneswar, India; Homi Bhabha National Institute, Training School Complex, Mumbai 400094, India;* orcid.org/0000-0001-9474-821X

María González-Viegas − *Institut für Biologie, Humboldt Universität zu Berlin, 10115 Berlin, Germany*

Complete contact information is available at: https://pubs.acs.org/10.1021/acscentsci.1c00768

Author Contributions

H.S.B. conceptualized the project. K.D.T. and S.J. performed the experiments and analyzed the data. M.G.-V. and R.K.K. carried out the computational modeling and simulations. The manuscript was written through the contributions of all authors. All authors have approved the final version of the manuscript.

Funding

K.D.T., S.J., and H.S.B. acknowledge financial support from the Department of Atomic Energy, Department of Science and Technology (Project File No. CRG/2018/000892), Government of India.

Notes

The authors declare no competing financial interest.

■ ACKNOWLEDGMENTS

This manuscript is dedicated to the 80th Birthday of Professor Anadi Charan Dash and the 65th Birthday of Professor Sanjay Wategaonkar. K.D.T., S.J., and H.S.B. acknowledge the Centre for Interdisciplinary Sciences (CIS), NISER for the experimental facilities.

■ REFERENCES

(1) Haque, F.; Pi, F.; Zhao, Z.; Gu, S.; Hu, H.; Yu, H.; Guo, P. RNA versatility, flexibility, and thermostability for practice in RNA nanotechnology and biomedical applications. *WIREs RNA* **2018**, *9*, No. e1452.

(2) Hu, X.-P.; Dourado, H.; Schubert, P.; Lercher, M. J. The protein translation machinery is expressed for maximal efficiency in Escherichia coli. *Nat. Commun.* **2020**, *11*, 5260.

(3) Di Giorgio, S.; Martignano, F.; Torcia, M. G.; Mattiuz, G.; Conticello, S. G. Evidence for host-dependent RNA editing in the transcriptome of SARS-CoV-2. *Sci. Adv.* **2020**, *6*, No. eabb5813.

(4) Guo, P. The emerging field of RNA nanotechnology. *Nat. Nanotechnol.* **2010**, *5*, 833−842.

(5) Remenyi, A.; Scholer, H. R; Wilmanns, M. Combinatorial control of gene expression. *Nat. Struct. Mol. Biol.* **2004**, *11*, 812−815.

(6) Chandramouly, G.; Zhao, J.; McDevitt, S.; Rusanov, T.; Hoang, T.; Borisonnik, N.; Treddinick, T.; Lopezcolorado, F. W.; Kent, T.; Siddique, L. A.; et al. Polθ reverse transcribes RNA and promotes RNA-templated DNA repair. *Sci. Adv.* **2021**, *7*, No. eabf1771.

(7) Mandal, A.; Kumbhojkar, N.; Reilly, C.; Dharamdasani, V.; Ukidve, A.; Ingber, D. E.; Mitragotri, S. Treatment of psoriasis with NFKBIZ siRNA using topical ionic liquid formulations. *Sci. Adv.* **2020**, *6*, No. eabb6049.

(8) Levy, M.; Miller, S. L. The stability of the RNA bases: Implications for the origin of life. *Proc. Natl. Acad. Sci. U. S. A.* **1998**, *95*, 7933−7938.

(9) Ma, S; Huang, Y; van Huystee, R.B Improved plant RNA stability in storage. *Anal. Biochem.* **2004**, *326*, 122−124.

(10) Fabre, A.-L.; Colotte, M.; Luis, A.; Tuffet, S.; Bonnet, J. An efficient method for long-term room temperature storage of RNA. *Eur. J. Hum. Genet.* **2014**, *22*, 379−385.

(11) Seelenfreund, E.; Robinson, W. A.; Amato, C. M.; Tan, A.-C.; Kim, J.; Robinson, S. E. Long Term Storage of Dry versus Frozen RNA for Next Generation Molecular Studies. *PLoS One* **2014**, *9*, No. e111827.

(12) Puddu, M.; Stark, W. J.; Grass, R. N. Silica Microcapsules for Long-Term, Robust, and Reliable Room Temperature RNA Preservation. *Adv. Healthcare Mater.* **2015**, *4*, 1332−1338.

(13) Tateishi-Karimata, H.; Sugimoto, N. Biological and nanotechnological applications using interactions between ionic liquids and nucleic acids. *Biophys. Rev.* **2018**, *10*, 931−940.

(14) Lei, Z.; Chen, B.; Koo, Y.-M.; MacFarlane, D. R. Introduction: Ionic Liquids. *Chem. Rev.* **2017**, *117*, 6633−6635.

(15) Greaves, T. L.; Drummond, C. J. Protic Ionic Liquids: Properties and Applications. *Chem. Rev.* **2008**, *108*, 206−237.

(16) Thoppil, A. A.; Chennuri, B. K.; Gardas, R. L. Insights into the structural changes of bovine serum albumin in ethanolammoniumlaurate based surface active ionic liquids. *J. Mol. Liq.* **2019**, *290*, 111229.

(17) Swatloski, R. P.; Spear, S. K.; Holbrey, J. D.; Rogers, R. D. Dissolution of Cellose with Ionic Liquids. *J. Am. Chem. Soc.* **2002**, *124*, 4974−4975.

(18) Sahoo, D. K.; Chand, A.; Jena, S.; Biswal, H. S. Hydrogen-bond-driven thiouracil dissolution in aqueous ionic liquid: A combined microscopic, spectroscopic and molecular dynamics study. *J. Mol. Liq.* **2020**, *319*, 114275.

(19) Sahoo, D. K.; Mundlapati, V. R.; Gagrai, A. A.; Biswal, H. S. Efficient SO_2 Capture through Multiple Chalcogen Bonds, Sulfur-Centered Hydrogen Bonds and S•••π Interactions: A Computational Study. *ChemistrySelect* **2016**, *1*, 1688−1694.

(20) Choi, Y. H.; Verpoorte, R. Green solvents for the extraction of bioactive compounds from natural products using ionic liquids and deep eutectic solvents. *Curr. Opin. Food Sci.* **2019**, *26*, 87−93.

(21) Clark, K. D.; Trujillo-Rodríguez, M. J.; Anderson, J. L. Advances in the analysis of biological samples using ionic liquids. *Anal. Bioanal. Chem.* **2018**, *410*, 4567−4573.

(22) Fister, S.; Fuchs, S.; Mester, P.; Kilpeläinen, I.; Wagner, M.; Rossmanith, P. The use of ionic liquids for cracking viruses for isolation of nucleic acids. *Sep. Purif. Technol.* **2015**, *155*, 38−44.

(23) Naushad, M.; Alothman, Z. A.; Khan, A. B.; Ali, M. Effect of ionic liquid on activity, stability, and structure of enzymes: A review. *Int. J. Biol. Macromol.* **2012**, *51*, 555−560.
(24) Kumar Sahoo, D.; Devi Tulsiyan, K.; Jena, S.; Biswal, H. S. Implication of Threonine-Based Ionic Liquids on the Structural Stability, Binding and Activity of Cytochrome c. *ChemPhysChem* **2020**, *21*, 2525−2535.
(25) Lin, Y.; Zhao, A.; Tao, Y.; Ren, J.; Qu, X. Ionic Liquid as an Efficient Modulator on Artificial Enzyme System: Toward the Realization of High-Temperature Catalytic Reactions. *J. Am. Chem. Soc.* **2013**, *135*, 4207−4210.
(26) Singh, S. K.; Savoy, A. W. Ionic liquids synthesis and applications: An overview. *J. Mol. Liq.* **2020**, *297*, 112038.
(27) Ventura, S. P. M.; E Silva, F. A.; Quental, M. V.; Mondal, D.; Freire, M. G.; Coutinho, J. A. P. Ionic-Liquid-Mediated Extraction and Separation Processes for Bioactive Compounds: Past, Present, and Future Trends. *Chem. Rev.* **2017**, *117*, 6984−7052.
(28) Sahoo, D. K.; Jena, S.; Tulsiyan, K. D.; Dutta, J.; Chakrabarty, S.; Biswal, H. S. Amino-Acid-Based Ionic Liquids for the Improvement in Stability and Activity of Cytochrome c: A Combined Experimental and Molecular Dynamics Study. *J. Phys. Chem. B* **2019**, *123*, 10100−10109.
(29) Benedetto, A.; Ballone, P. Room Temperature Ionic Liquids Meet Biomolecules: A Microscopic View of Structure and Dynamics. *ACS Sustainable Chem. Eng.* **2016**, *4*, 392−412.
(30) Pabbathi, A.; Samanta, A. On the Stability and Conformational Dynamics of Cytochrome c in Ammonium Ionic Liquids. *J. Phys. Chem. B* **2020**, *124*, 8132−8140.
(31) Egorova, K. S; Posvyatenko, A. V; Larin, S. S; Ananikov, V. P Ionic liquids: prospects for nucleic acid handling and delivery. *Nucleic Acids Res.* **2021**, *49*, 1201−1234.
(32) Chandran, A.; Ghoshdastidar, D.; Senapati, S. Groove Binding Mechanism of Ionic Liquids: A Key Factor in Long-Term Stability of DNA in Hydrated Ionic Liquids? *J. Am. Chem. Soc.* **2012**, *134*, 20330−20339.
(33) Sahoo, D. K.; Jena, S.; Dutta, J.; Chakrabarty, S.; Biswal, H. S. Critical Assessment of the Interaction between DNA and Choline Amino Acid Ionic Liquids: Evidences of Multimodal Binding and Stability Enhancement. *ACS Cent. Sci.* **2018**, *4*, 1642−1651.
(34) Zhao, H. DNA stability in ionic liquids and deep eutectic solvents. *J. Chem. Technol. Biotechnol.* **2015**, *90*, 19−25.
(35) Pabbathi, A.; Samanta, A. Spectroscopic and Molecular Docking Study of the Interaction of DNA with a Morpholinium Ionic Liquid. *J. Phys. Chem. B* **2015**, *119*, 11099−11105.
(36) Ghoshdastidar, D.; Senapati, S. Dehydrated DNA in B-form: ionic liquids in rescue. *Nucleic Acids Res.* **2018**, *46*, 4344−4353.
(37) Brisco, M. J.; Morley, A. A. Quantification of RNA integrity and its use for measurement of transcript number. *Nucleic Acids Res.* **2012**, *40*, No. e144.
(38) Mamajanov, I.; Engelhart, A. E.; Bean, H. D.; Hud, N. V. DNA and RNA in Anhydrous Media: Duplex, Triplex, and G-Quadruplex Secondary Structures in a Deep Eutectic Solvent. *Angew. Chem., Int. Ed.* **2010**, *49*, 6310−6314.
(39) Mazid, R. R.; Divisekera, U.; Yang, W.; Ranganathan, V.; MacFarlane, D. R.; Cortez-Jugo, C.; Cheng, W. Biological stability and activity of siRNA in ionic liquids. *Chem. Commun.* **2014**, *50*, 13457−13460.
(40) Pedro, A. Q.; Pereira, P.; Quental, M. J.; Carvalho, A. P.; Santos, S. M.; Queiroz, J. A.; Sousa, F.; Freire, M. G. Cholinium-Based Good's Buffers Ionic Liquids as Remarkable Stabilizers and Recyclable Preservation Media for Recombinant Small RNAs. *ACS Sustainable Chem. Eng.* **2018**, *6*, 16645−16656.
(41) Quental, M. V.; Pedro, A. Q.; Pereira, P.; Sharma, M.; Queiroz, J. A.; Coutinho, J. A. P.; Sousa, F.; Freire, M. G. Integrated Extraction-Preservation Strategies for RNA Using Biobased Ionic Liquids. *ACS Sustainable Chem. Eng.* **2019**, *7*, 9439−9448.
(42) Boo, S. H.; Kim, Y. K. The emerging role of RNA modifications in the regulation of mRNA stability. *Exp. Mol. Med.* **2020**, *52*, 400−408.
(43) Biver, T. Use of UV-Vis Spectrometry to Gain Information on the Mode of Binding of Small Molecules to DNAs and RNAs. *Appl. Spectrosc. Rev.* **2012**, *47*, 272−325.
(44) Gatti, C.; Houssier, C.; Fredericq, E. Binding of ethidium bromide to ribosomal RNA. Absorption, fluorescence, circular and electric dichroism study. *Biochim. Biophys. Acta, Nucleic Acids Protein Synth.* **1975**, *407*, 308−319.
(45) Cui, H. H.; Valdez, J. G.; Steinkamp, J. A.; Crissman, H. A. Fluorescence lifetime-based discrimination and quantification of cellular DNA and RNA with phase-sensitive flow cytometry. *Cytometry* **2003**, *52A*, 46−55.
(46) Šponer, J.; Bussi, G.; Krepl, M.; Banáš, P.; Bottaro, S.; Cunha, R. A.; Gil-Ley, A.; Pinamonti, G.; Poblete, S.; Jurečka, P.; et al. RNA Structural Dynamics As Captured by Molecular Simulations: A Comprehensive Overview. *Chem. Rev.* **2018**, *118*, 4177−4338.
(47) Gendron, P.; Lemieux, S.; Major, F. Quantitative analysis of nucleic acid three-dimensional structures11Edited by I. Tinoco. *J. Mol. Biol.* **2001**, *308*, 919−936.
(48) Bottaro, S.; Di Palma, F.; Bussi, G. The role of nucleobase interactions in RNA structure and dynamics. *Nucleic Acids Res.* **2014**, *42*, 13306−13314.
(49) Kührová, P.; Banáš, P.; Best, R. B.; Šponer, J.; Otyepka, M. Computer Folding of RNA Tetraloops? Are We There Yet? *J. Chem. Theory Comput.* **2013**, *9*, 2115−2125.
(50) Bernacchi, S. In *RNA Spectroscopy: Methods and Protocols*; Arluison, V.; Wien, F., Eds.; Springer: New York, NY, 2020, DOI: 10.1007/978-1-0716-0278-2_4.
(51) Borodavka, A.; Singaram, S. W.; Stockley, P. G.; Gelbart, W. M.; Ben-Shaul, A.; Tuma, R. Sizes of Long RNA Molecules Are Determined by the Branching Patterns of Their Secondary Structures. *Biophys. J.* **2016**, *111*, 2077−2085.
(52) Harvey, J. D. Diffusion coefficients and hydrodynamic radii of three spherical RNA viruses by laser light scattering. *Virology* **1973**, *56*, 365−368.
(53) Wu, P.; Nakano, S.-i.; Sugimoto, N. Temperature dependence of thermodynamic properties for DNA/DNA and RNA/DNA duplex formation. *Eur. J. Biochem.* **2002**, *269*, 2821−2830.
(54) Puglisi, J. D.; Tinoco, I. Absorbance melting curves of RNA. *Meth. Enzymol.* **1989**, *180*, 304−325.
(55) Moore, D. S.; Wagner, T. E. Origins of the differences between the circular dichroism of DNA and RNA: Theoretical calculations. *Biopolymers* **1973**, *12*, 201−221.
(56) Petkovic, M.; Ferguson, J. L.; Gunaratne, H. Q. N.; Ferreira, R.; Leitão, M. C.; Seddon, K. R.; Rebelo, L. P. N.; Pereira, C. S. Novel biocompatible cholinium-based ionic liquids—toxicity and biodegradability. *Green Chem.* **2010**, *12*, 643−649.
(57) Pernak, J.; Syguda, A.; Mirska, I.; Pernak, A.; Nawrot, J.; Pradzýska, A.; Griffin, S. T.; Rogers, R. D. Choline-Derivative-Based Ionic Liquids. *Chem. - Eur. J.* **2007**, *13*, 6817−6827.
(58) Mishra, A.; Ekka, M. K.; Maiti, S. Influence of Ionic Liquids on Thermodynamics of Small Molecule−DNA Interaction: The Binding of Ethidium Bromide to Calf Thymus DNA. *J. Phys. Chem. B* **2016**, *120*, 2691−2700.
(59) Docherty, K. M.; Kulpa, C. F., Jr. Toxicity and antimicrobial activity of imidazolium and pyridinium ionic liquids. *Green Chem.* **2005**, *7*, 185−189.
(60) Sharma, M.; Mondal, D.; Singh, N.; Trivedi, N.; Bhatt, J.; Prasad, K. High concentration DNA solubility in bio-ionic liquids with long-lasting chemical and structural stability at room temperature. *RSC Adv.* **2015**, *5*, 40546−40551.
(61) Bisht, M.; Venkatesu, P. Influence of cholinium-based ionic liquids on the structural stability and activity of α-chymotrypsin. *New J. Chem.* **2017**, *41*, 13902−13911.
(62) Cho, C.-W.; Pham, T. P. T.; Zhao, Y.; Stolte, S.; Yun, Y.-S. Review of the toxic effects of ionic liquids. *Sci. Total Environ.* **2021**, *786*, 147309.
(63) Zakrewsky, M.; Mitragotri, S. Therapeutic RNAi robed with ionic liquid moieties as a simple, scalable prodrug platform for treating skin disease. *J. Controlled Release* **2016**, *242*, 80−88.

https://doi.org/10.1021/acscentsci.1c00768
ACS Cent. Sci. 2021, 7, 1688−1697

(64) Dharamdasani, V.; Mandal, A.; Qi, Q. M.; Suzuki, I.; Bentley, M. V. L. B.; Mitragotri, S. Topical delivery of siRNA into skin using ionic liquids. *J. Controlled Release* **2020**, *323*, 475−482.
(65) Ohno, H.; Fukumoto, K. Amino Acid Ionic Liquids. *Acc. Chem. Res.* **2007**, *40*, 1122−1129.

https://doi.org/10.1021/acscentsci.1c00768
ACS Cent. Sci. 2021, 7, 1688−1697